Journal of Inorganic and General Chemistry
ZAAC
Zeitschrift für anorganische und allgemeine Chemie
www.zaac.wiley-vch.de
RESEARCH ARTICLE
DOI: 10.1002/zaac.202200209

Exchange of ammine- and fluorido-ligands in complex salts: The series $[Cr(NH_3)_6][AlF_6]$, $[Cr(NH_3)_5F][SiF_6]$ and $K_2[Cr(NH_3)_4F_2][Si(NH_3)_{0.5}F_{5.5}]_2$

Christian Bäucker[a] and Rainer Niewa*[a]

Dedicated to Prof. Dr. Wolfgang Schnick on the occasion of his 65th birthday

The three amminechromium(III) complex compounds $[Cr(NH_3)_6][AlF_6]$, $[Cr(NH_3)_5F][SiF_6]$ and $K_2[Cr(NH_3)_4F_2][Si(NH_3)_{0.5}F_{5.5}]_2$ were obtained from ammonothermal synthesis at $T_{max}=724$ K and $p_{max}=2120$ bar. Crystal structures were determined from single crystal X-ray diffraction. The gradual exchange of ammine ligands by fluoride ligands in the amminechromium(III) ions is reflected by an intriguing change in color. The mutual ligand exchange between ammonia ligands and fluoride ions occurs in both the cations and the anions, indicating the various dissolved species present under the synthetic conditions.

Introduction

Ammonothermal synthesis was originally developed as a synthetic tool to address mostly novel amides and nitrides with special focus on their crystal growth for structural elucidation by the pioneer in this field Herbert Jacobs.[1] After successful growth of high quality III-nitride crystals,[2,3] recently a revival in exploring this experimental technique and possible product materials began. One relevant research direction was the ammonothermal synthesis of nitridosilicates by Wolfgang Schnick et al., particularly known for their superior luminescence properties.[4] However, growth of larger crystals of such materials so far remains elusive, possibly due to low solubility of silicon under most ammonothermal conditions. Earlier, we have observed the formation and crystal growth of hexafluoridosilicates and -aluminates from supercritical ammonia in presence of fluoride ions. Now we present further information on solid compounds of silicon and aluminium obtained from ammonothermal synthesis, indicating the nature of various dissolved species present under the given conditions.[5,6] Particularly intriguing is the successive interexchange of ammine and fluoride ligands on both the cationic and the anionic complex ions in the title compounds. The observation of a complex ion involving a bond between nitrogen and silicon may lead a way to future crystal growth of nitridosilicates from supercritical ammonia in presence of fluoride ions.

[a] Dr. C. Bäucker, Prof. Dr. R. Niewa
Institute of Inorganic Chemistry
University of Stuttgart
Pfaffenwaldring 55, 70569 Stuttgart, Germany
E-mail: rainer.niewa@iac.uni-stuttgart.de

Supporting information for this article is available on the WWW under https://doi.org/10.1002/zaac.202200209

Results and Discussion

All three title compounds were obtained from reaction of CrF_3 in presence of KNH_2 and NH_4F with the crucible material (sintered Si_3N_4 with small amounts of Al_2O_3 added as sinter-aid) under ammonothermal conditions at $T_{max}=724$ K and $p_{max}=2120$ bar. The product crystals were obtained from the hotter zone at the bottom of the autoclave within an intended thermal gradient, indicating so-called retrograde solubilities, i.e. lower solubility at higher temperatures typically found for ammonobasic growth of GaN crystals, to name only one prominent example.[3] We have observed earlier that both aluminium and silicon are dissolved from the crucible material under the applied conditions in presence of fluoride ions as fluoridoaluminate and -silicate ions and also isolated the products from the hot zone of the autoclave.[5,6]

The three title compounds, hexaamminechromium(III) hexafluoridoaluminate(III), $[Cr(NH_3)_6][AlF_6]$, pentaamminemonofluoridochromium(III) hexafluoridosilicate(IV), $[Cr(NH_3)_5F][SiF_6]$ and dipotassium tetraamminedifluoridochromium(III) bis(hemiamminehemipentafluoridosilicate(IV)), $K_2[Cr(NH_3)_4F_2][Si(NH_3)_{0.5}F_{5.5}]_2$ are easily distinguished on a macroscopic level by the shape and color of their crystals (see Figure 1). $[Cr(NH_3)_6][AlF_6]$ forms bright orange crystals, $[Cr(NH_3)_5F][SiF_6]$ dark red crystals and $K_2[Cr(NH_3)_4F_2][Si(NH_3)_{0.5}F_{5.5}]_2$ crystallizes as rose colored plates in agreement with its tetragonal space group symmetry. All three compounds proofed to be stable in air for at least several days without any apparent change in color or appearance, which we associate with some effective stabilization by hydrogen bonding as discussed below.

Table 1. Selected crystallographic parameters and refinement data of $[Cr(NH_3)_6][AlF_6]$, $[Cr(NH_3)_5F][SiF_6]$ and $K_2[Cr(NH_3)_4F_2][Si(NH_3)_{0.5}F_{5.5}]_2$.

Composition	$[Cr(NH_3)_6]$ $[AlF_6]$	$[Cr(NH_3)_5F]$ $[SiF_6]$	$K_2[Cr(NH_3)_4F_2]$ $[Si(NH_3)_{0.5}F_{5.5}]_2$
Crystal system	Cubic	Monoclinic	Tetragonal
Space group	$Pa\bar{3}$	$P2_1/c$	$I4/m$
a/pm	998.62(4)	1458.74(5)	607.55(3)
b/pm	–	1017.94(6)	–
c/pm	–	1379.33(5)	2115.12(13)
β/°	–	90.851(3)	–
Z	4	8	2
Density (calculated)/ $g\cdot cm^{-3}$	1.969	1.922	2.125
Volume/10^6 pm^3	995.87	2047.95	780.73
Index ranges hkl	$-11 \le h \le 12$ $-12 \le k \le 10$ $-12 \le l \le 12$	$-21 \le h \le 21$ $-15 \le k \le 15$ $-20 \le l \le 20$	$-7 \le h \le 7$ $-7 \le k \le 7$ $-26 \le l \le 27$
$2\theta_{max}$/°	54.93	63.86	55.74
$F(000)$	604	1208	482
μ(Mo-$K_{\alpha1}$)/mm^{-1}	1.30	1.31	1.55
Measured reflections/ sym. independent	5996/356	73423/6764	5769/481
R_{int}/R_σ	0.0959/0.0279	0.0933/0.0804	0.0743/0.0398
R_1 with $\lvert F_o\rvert > 4\sigma(F_o)$, observed reflections	0.0437, 286	0.0446, 3950	0.0459, 386
$R_1/wR_2/GooF$	0.0593/0.1120/1.238	0.1057/0.1279/1.080	0.0588/0.1407/1.007
Largest peak/hole in the difference electron density map/10^6 pm^{-3}	0.79/−0.46	0.45/−0.56	0.96/−0.48
BASF		0.0788(9)	0.488(9)
Twin matrix	–	$\begin{pmatrix} 1 & 0 & 0 \\ 0 & \bar{1} & 0 \\ 0 & 0 & \bar{1} \end{pmatrix}$	$\begin{pmatrix} 1 & 0 & 0 \\ 0 & \bar{1} & 0 \\ 0 & 0 & \bar{1} \end{pmatrix}$

$[Cr(NH_3)_6][AlF_6]$

Chromium and aluminium in the crystal structure of $[Cr(NH_3)_6][AlF_6]$ are both coordinated octahedrally, forming mutually isolated complex ions. The crystal structure is most accurately described as a hierarchical variant of the rocksalt type, with the complex units $[Cr(NH_3)_6]^{3+}$ and $[AlF_6]^{3-}$ replacing the monoatomic ions of the aristotype. Selected structure refinement data are given in Table 1. Additional information on fractional atomic coordinates and displacement parameters can be found in the supplementary material, Tables S1 and S2. This compound was already reported by Wieghart *et al.* in 1971 discussing mostly unit cell parameters and spectroscopic investigations.[7] One year later, the crystal structures of the isotypic compounds $[Cr(NH_3)_6][FeF_6]$ and $[Cr(NH_3)_6][MnF_6]$ were reported.[8] Recently, we obtained the isotypic $[In(NH_3)_6][AlF_6]$ from near-neutral ammonothermal synthesis in presence of fluoride ions.[5]

The expanded unit cell of $[Cr(NH_3)_6][AlF_6]$ emphasizing the octahedral coordination spheres of both chromium and aluminium atoms is displayed in Figure 2. The high space group symmetry $Pa\bar{3}$ results in six identical distances in each complex ion (d(Cr–N) = 207.8(3) pm and d(Al–F) = 181.4(2) pm), within the typical range for such complex ions (for full distance and angle information see supplementary material, Table S3). Angles within the octahedra are close to the ideal 90°, with a somewhat larger deviation for the hexaamminechromium(III) ion than for the hexafluoridoaluminate(III) ion. Microprobe chemical analysis on this type of crystals indicated the presence of the assigned elements (except for hydrogen due to detection limits).

For $[Cr(NH_3)_6][AlF_6]$, we were able to take the positions of the hydrogen atoms from the electron difference map and refine those without constraints except for the isotropic displacement parameters restricted to 1.2 times of the nitrogen atom attached to. This knowledge of hydrogen atom positions enables us to analyze the hydrogen bonding network occurring between the ammine ligands as donors and the fluorido ligands

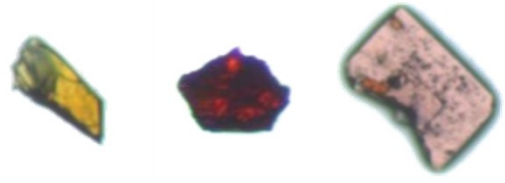

Figure 1. Crystals of $[Cr(NH_3)_6][AlF_6]$ (orange, left), $[Cr(NH_3)_5F_2][SiF_6]$ (dark red, middle) and $K_2[Cr(NH_3)_4F_2][Si(NH_3)_{0.5}F_{5.5}]_2$ (rose, right) as seen under a microscope. All compounds were present in the product in roughly equal amounts.

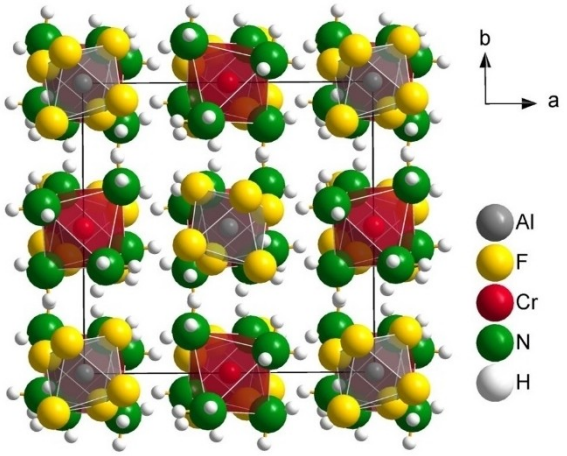

Figure 2. Extended unit cell of $[Cr(NH_3)_6][AlF_6]$. The octahedra around chromium and aluminium are shown in red and grey respectively, the unit cell is indicated.

of adjacent anions as acceptors: The surrounding of a $[Cr(NH_3)_6]^{3+}$ complex ion by $[AlF_6]^{3-}$ octahedra is shown in Figure 3, indicating possible hydrogen bonds a dashed lines. The interatomic distances in the range of d(H···F) = 200(4)–212(5) pm and d(N–F) = 294(4)–301(4) pm indicate rather moderate strength of the hydrogen bonds, as the donor-acceptor distances are only slightly shorter than the sum of the van-der-Waals radii with 302 pm.[9,10] Additionally, the angles at the bridging hydrogen atoms with 145°–161° significantly deviate from 180°. Still, this compound proofed to be stable in air for at least several days without any apparent change in color or appearance, which might be associated with some effective stabilization by weak hydrogen bonding.

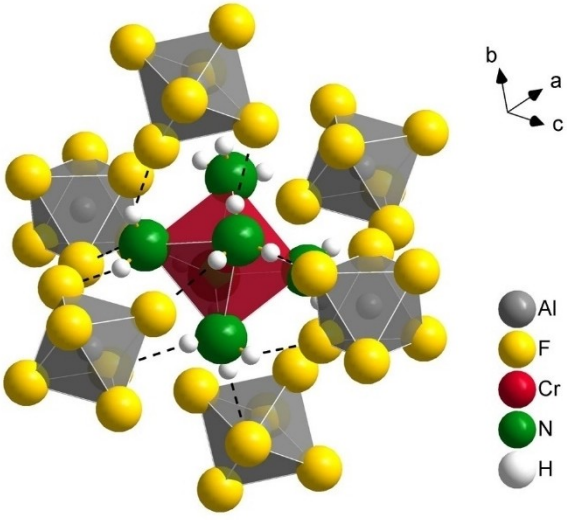

Figure 3. Hydrogen bonding framework between ammonia groups of $[Cr(NH_3)_6]^{3+}$ ions (red octahedron) and fluorido ligands of $[AlF_6]^{3-}$ ions (grey octahedra) in $[Cr(NH_3)_6][AlF_6]$.

$[Cr(NH_3)_5F][SiF_6]$

$[Cr(NH_3)_5F][SiF_6]$ crystallizes in the monoclinic space group $P2_1/c$. All crystals studied turned out to suffer from twinning according to the twin matrix displayed in Table 1. For fractional atomic coordinates and displacement parameters compare the supplementary data, Tables S4 and S5.

Upon detailed evaluation of distances within the two crystallographic independent complex cations, one distance between chromium and a ligand in each turned out to be significantly shorter with 186.3(2) and 187.0(2) pm than the remaining five distances d(Cr–N) = 206.3(3)–210.0(3) pm, which fall well within the expected range. This about 20 pm shorter distance is a clear indicator of substitution of an ammonia molecule in $[Cr(NH_3)_6]^{3+}$ to give the double positively charged ion $[Cr(NH_3)_5F]^{2+}$. Formation of mixed amminefluoridochromium(III) ions was earlier observed. For example $[Cr(NH_3)_4F_2]I \cdot H_2O$, cis-$[Cr(NH_3)_4F_2]ClO_4$ and $[Cr(NH_3)_6][Cr(NH_3)_2F_4][BF_4]_2$ exhibit very similar distances with d(Cr–N) = 205.1–208.7 pm and d(Cr–F) = 188.7–189.4(3) pm.[11] The charge of the $[Cr(NH_3)_5F]^{2+}$ ion in this title compound is balanced by an octahedral $[SiF_6]^{2-}$ ion, supported by the short distances d(Si–F) = 166.3(2)–169.8(2) pm (for full distance and angle information compare supplementary material, Table S6). Microprobe chemical analysis on crystals of this type revealed the exclusive presence of the assigned elements (except for hydrogen due to detection limits). Again, the mutually isolated complex ions in $[Cr(NH_3)_5F][SiF_6]$ arrange in a hierarchical structural variant of the rocksalt type, visible when consulting the extended unit cell (Figure 4).

However, one important difference occurs: While all fluoride ligands of the octahedral $[SiF_6]^{2-}$ ion are involved in hydrogen bonds with ammine ligands of the $[Cr(NH_3)_5F]^{2+}$ ion (d(F–N) = 288.7(5)–300.6(5) pm), the fluoride ligand of the latter cation bridges to two adjacent ammonia groups of complex cations, by this realizing infinite chains running parallel to the crystallographic a-axis (d(F–N) = 286.3(5)–295.7(5) pm, see Figures 5 and 6). The formation of these chains causes a further symmetry reduction and deformation with respect to the rocksalt aristotype.

Again, we associate the stability in air for at least several days without any apparent change in color or appearance with a stabilizing effect of the hydrogen bonding network.

$K_2[Cr(NH_3)_4F_2][Si(NH_3)_{0.5}F_{5.5}]_2$

The tetragonal crystal structure of $K_2[Cr(NH_3)_4F_2][Si(NH_3)_{0.5}F_{5.5}]_2$ constitutes from complex ions $[Cr(NH_3)_4F_2]^+$ next to $[Si(NH_3)_{0.5}F_{5.5}]^{1.5-}$ (in average) with additional potassium cations intercalated between layers of the latter ions (see Figure 7). In the derived space group $I4/m$, the complex cations feature exclusively ammine ligands at axial positions and rotational disorder parallel [001] superposing same numbers of ammine and fluoride ligands at the four equatorial positions. For the anions apparently equal numbers of $[SiF_6]^{2-}$ and $[Si(NH_3)F_5]^{1-}$ ions can statistically replace each other for charge balance.

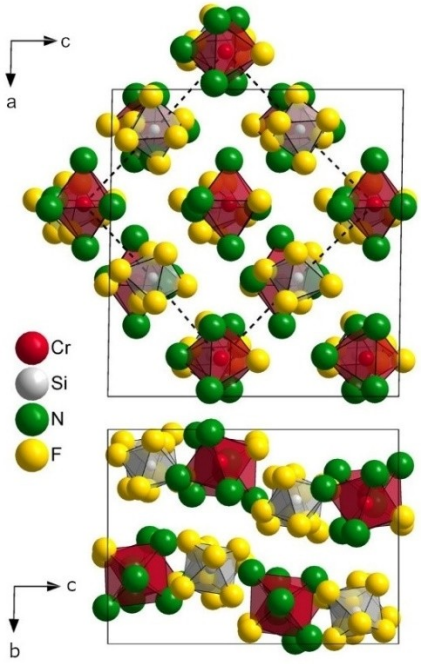

Figure 4. Extended unit cell of $[Cr(NH_3)_5F][SiF_6]$ viewed along the crystallographic *b*-axis (top) and the *c*-axis (bottom). The octahedral surroundings of Si and Cr atoms are displayed in grey and red, respectively. The unit cell edges are displayed. In the upper figure, the underlying *fcc*-cell of the aristotype is indicated by dashed lines.

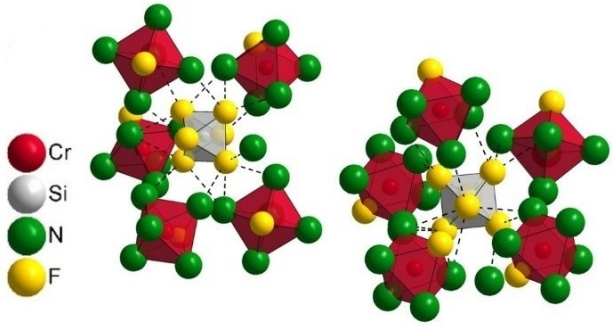

Figure 5. Hydrogen bonds between $[SiF_6]^{2-}$ (grey) and $[Cr(NH_3)_5F]^{2+}$ (red) complex ions in $[Cr(NH_3)_5F][SiF_6]$. For clarity, only two- and three-dentate $[Cr(NH_3)_5F]^{2+}$ ions are fully depicted, monodentate coordinating complex ions are only represented by the coordinating fluorido ligand.

Symmetry reduction does not lead to any ordered structure model in agreement with the diffraction data. Information on structure determination are gathered in Table 1, fractional coordinates and displacement parameters in the supplementary material, Tables S7 and S8. Microprobe chemical analyses on these types of crystals again did not indicate the presence any further elements than given in the sum formula.

Firstly focusing on the $[Cr(NH_3)_4F_2]^+$ ion, two longer distances d(Cr–N) = 207.2(7) pm occur, well in the range

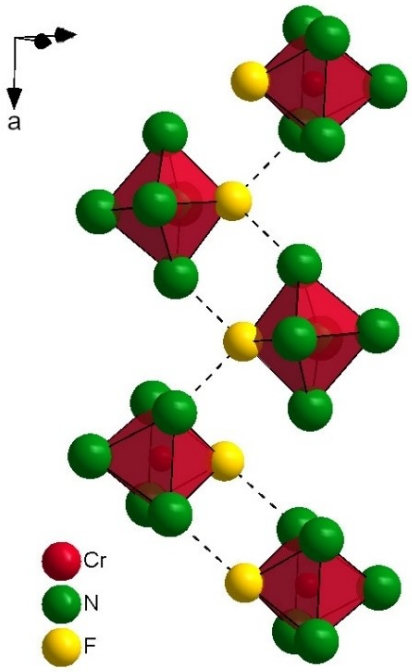

Figure 6. Hydrogen bonds between $[Cr(NH_3)_5F]^{2+}$ cations in $[Cr(NH_3)_5F][SiF_6]$.

observed within the above discussed structures. Four conspicuous slightly shorter distances d(Cr–N/F) = 196.8(6) pm surprise (for full distance and angle information see supplementary material, Table S9), too short for Cr–N but too long for Cr–F, indicating disorder of these two ligands. This assignment is supported by the hydrogen bonding network discussed below. We now turn to the $[Si(NH_3)_{0.5}F_{5.5}]^{1.5-}$ ions, which locally are represented by either $[SiF_6]^{2-}$ or $[Si(NH_3)F_5]^-$ ions. Again, within the octahedra we find five distances d(Si–F) = 166.7(3)–167.7(6) pm in the typical range and one suspiciously long distance d(Si–F/N) = 181.4(6) pm indicating partial substitution of the fluoride by ammine ligands. This latter distance is located well between those for Si–F and Si–N, for example, in the fully ordered ammonium monoamminepentafluoridosilicate(IV) $NH_4[Si(NH_3)F_5]$ with d(Si–N) = 167.8 pm and d(Si–F) = 190.0 pm.[12]

The locations of fluorido and ammine ligands in both complex ions are well reflected in the hydrogen bonding network. Again focusing on the octahedral coordination polyhedra around chromium firstly, these are turned around the *c*-axis by about 23.8° in order to provide short distances of 294.7(1) pm, shorter than the sum of van-der-Waals radii of 302 pm for N and F, between disordered ammine and fluorido ligands located at the equatorial positions and indicating the presence of hydrogen bonds.[9,10] For same ligands, however, this leaves ample space with distances of 361.8(1) pm to avoid each other (compare Figure 8).

This arrangement suggests local ordering of exclusively trans forms of the complex ion. However, from diffraction data refinements, we could not take any evidence for order of these ligands within this plane via symmetry reduction. Furthermore,

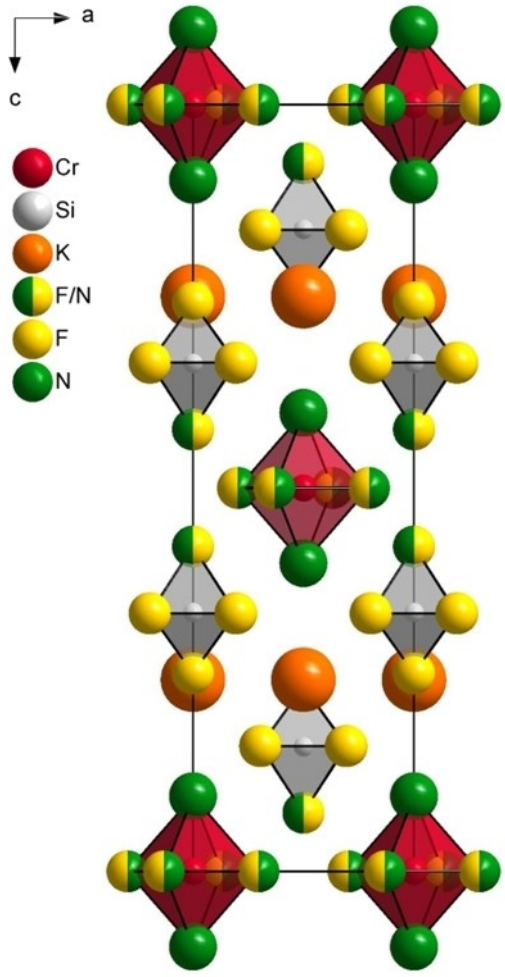

Figure 7. Extended unit cell of $K_2[Cr(NH_3)_4F_2][Si(NH_3)_{0.5}F_{5.5}]_2$. The coordination spheres of Cr^{3+} and Si^{4+} are displayed in red and grey, respectively. The unit cell edges are shown in black.

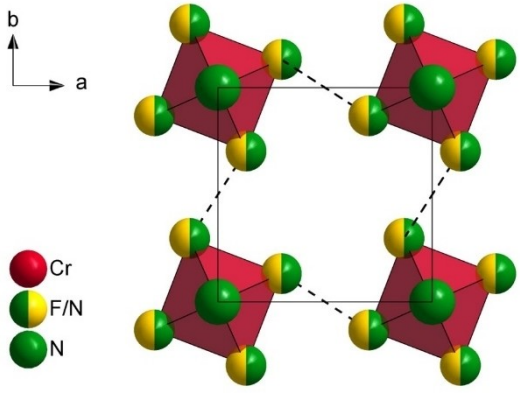

Figure 8. Hydrogen bonds between NH_3/F^- mixed sites of the coordination spheres around chromium in $K_2[Cr(NH_3)_4F_2][Si(NH_3)_{0.5}F_{5.5}]_2$.

the disordered equatorial ligands of the octahedral coordination surrounding chromium exhibit distances of 302.61(1) pm to the likewise with ammine and fluorido ligands occupied axial positions of the octahedral coordination of silicon (Figure 9). The purely by ammine ligands occupied axial positions of the octahedral coordination of chromium, however, are exclusively coordinated to four solely by fluoride occupied vertices of the octahedral coordination of silicon with distances of 297.1(4) pm (see Figure 10).

The equatorial fluoride positions of the octahedral surrounding of silicon in turn connect to one (axial) purely ammonia group of one $[Cr(NH_3)_4F_2]^+$ ion each (297.1(4) pm), while the mixed occupied position links to four equatorial mixed occupied ligands (F^-/NH_3) of these four complex cations with a distance of 302.61(1) pm (see Figure 11). Remarkably, the purely fluorido axial ligand in trans position to the mixed

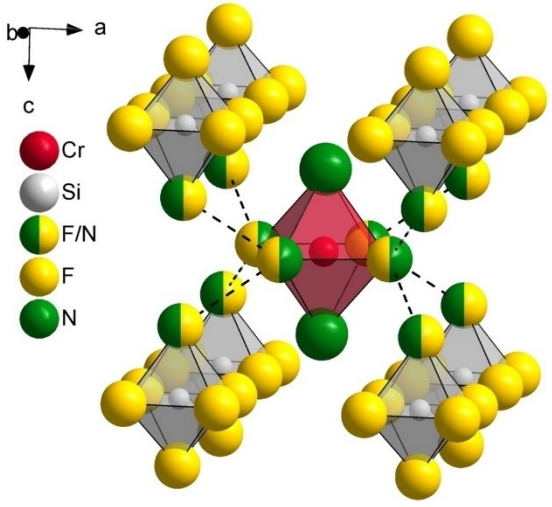

Figure 9. Hydrogen bonds between equatorial mixed NH_3/F^- ligands of $[Cr(NH_3)_4F_2]^+$ (red octahedron) and axial mixed sites of $[Si(NH_3)_{0.5}F_{5.5}]^{1.5-}$ (grey octahdra) in $K_2[Cr(NH_3)_4F_2][Si(NH_3)_{0.5}F_{5.5}]_2$ indicated by dashed lines.

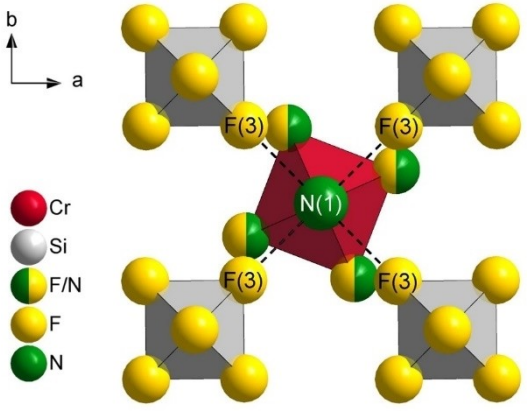

Figure 10. Hydrogen bonds between axial NH_3 ligands in the coordination sphere of $[Cr(NH_3)_4F_2]^+$ (red octahedron) and equatorial fluoride ligands in the coordination sphere of $[Si(NH_3)_{0.5}F_{5.5}]^{1.5-}$ (grey octahedra) in $K_2[Cr(NH_3)_4F_2][Si(NH_3)_{0.5}F_{5.5}]_2$ indicated by dashed lines.

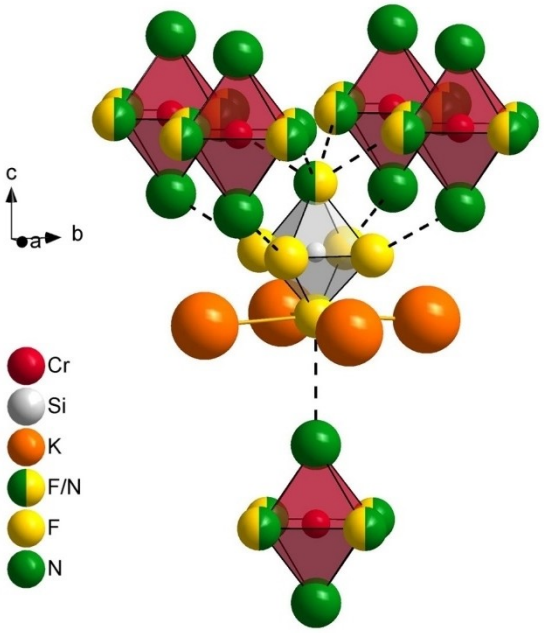

Figure 11. Surrounding of the $[Si(NH_3)_{0.5}F_{5.5}]^{1.5-}$ ion (grey octahedron) by $[Cr(NH_3)_4F_2]^+$ ions (red octahedra) and potassium ions (orange spheres) in $K_2[Cr(NH_3)_4F_2][Si(NH_3)_{0.5}F_{5.5}]_2$ and hydrogen bonding framework indicated by dashed lines.

occupied position only has one long distance of >338 pm to the next ammine ligand, but is coordinated by four potassium ions within a square.

The potassium ions in turn are exclusively coordinated by fluorido ligands attached to silicon atoms in a tetragonally distorted cuboctahedron with a typical range of distances of d(K–F) = 285.7(5)–304.28(3) pm (Figure 12). The distortion originates in the triangular faces with an edge-length defined by the rigid $[Si(NH_3)_{0.5}F_{5.5}]^{1.5-}$ complex ions, smaller than the remaining triangular faces. Similar distortions can be observed for example for the coordination of potassium ions in $K_2[SiF_6]$,[13] or in the better known isotypic $K_2[PtCl_6]$ (but here considerably less pronounced due to the larger chlorido ligands). Still, the coordination of the potassium ions in the title compound again underlines the close structural relation to the simple rocksalt aristotype.

Finally, we again associate the stability in air with the intriguing hydrogen bonding framework.

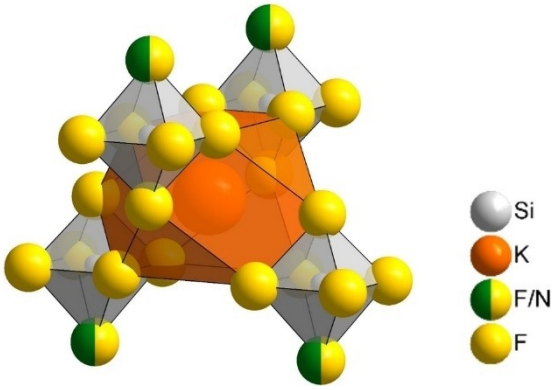

Figure 12. Surrounding of potassium ions (orange spheres) by $[Si(NH_3)_{0.5}F_{5.5}]^{1.5-}$ ions (grey octahedra) in $K_2[Cr(NH_3)_4F_2][Si(NH_3)_{0.5}F_{5.5}]_2$, resulting in a tetragonally distorted cuboctahedron.

Conclusions

We present three amminechromium(III) complex compounds obtained from ammonothermal synthesis showing an increasing exchange of ammine ligands by fluorido ligands coupled with an intriguing change in color. The colors reach from bright orange for $[Cr(NH_3)_6][AlF_6]$ over dark red for $[Cr(NH_3)_5F][SiF_6]$ to rose for $K_2[Cr(NH_3)_4F_2][Si(NH_3)_{0.5}F_{5.5}]_2$ (see Figure 1). The change in color from orange to a dark red for the hexaammine- and pentaamminemonofluoridochrom(III) complexes is obviously a result of exchange of the strong-field ligand ammonia to the weak-field ligand fluoride coupled with the loss of inversion symmetry causing the deepening in color. In $K_2[Cr(NH_3)_4F_2][Si(NH_3)_{0.5}F_{5.5}]_2$ the trend to smaller ligand field spitting is continued due to the double exchange of ammonia by fluoride ions in the coordination environment of chromium, however, an inversion center in the resulting ion is restored leading to least effective electronic transitions and thus less color intensity.

The ligand exchange from ammonia molecules to fluoride ions in the cations is accompanied by an exchange of fluorido by ammine ligands in the rather stable hexafluoridosilicate(IV) anion in $K_2[Cr(NH_3)_4F_2][Si(NH_3)_{0.5}F_{5.5}]_2$, indicating a whole zoo of dissolved ionic species present under ammonothermal conditions in various chemical equilibria. Interactions of these dissolved species and their influence on precipitated solid products are crucial for understanding of semiconductor formation and product quality. Furthermore, the presented observations might be the first steps for targeted nitridosilicate crystal growth from ammonothermal conditions and for targeted doping of main group III-nitride crystals with silicon atoms on the one hand and magnetic transition metal ions on the other hand.

Experimental Section

As some of the starting materials are sensitive towards air and moisture, the handling of both starting materials and products was done in an argon-filled glovebox (MBraun, Garching, Germany, $p(O_2) < 0.1$ ppm). For synthesis, custom-made autoclaves from nickel-based alloy 718 equipped with a pressure-transmitter to monitor the pressure inside (HBM P2VA2 and DA 2510, Hottinger Brüel & Kjaer, Darmstadt, Germany) and a burst disc holder (Type 750.5022-2, Alloy 718, SITEC-Sieber AG, Maur, Switzerland) were employed.[14,15] A custom-made Si_3N_4 liner (air-pressure sintered silicon nitride, Ingenieurkeramik, a QSIL company, Frankenblick, Germany) fitting inside the autoclave was used to protect the autoclave walls from corrosion induced by the used chemicals.[15,16] Additionally, a further, smaller Si_3N_4 crucible with a small lid was

placed within the liner to spatially separate starting materials and reduce transport rates within the supercritical fluid. Crucible and liner reduced the total volume of the reaction vessel from 98 ml to approximately 35 ml. After filling the autoclave with the starting materials inside the glovebox, closing and cooling with an ethanol-dry ice bath, a tensieudiometer after Hüttig was used to condense the desired amount of ammonia into the reaction vessel.[17] For heating, the autoclave was positioned upright in a tube furnace (LOBA 1200-60-400-1 OW, HTM Reetz, Berlin, Germany) with the autoclave top and installations outside the furnace. This causes a temperature gradient of approximately 100 K between bottom (hot zone) and top of the vessel (cold zone). After reaction, excess ammonia is released and the autoclave is brought back into the glovebox to recover the products.

As starting materials, gallium (100.61 mg; 1.443 mmol), CrF_3 (157.3 mg; 1.443 mmol) and NH_4F (160.3 mg; 4.329 mmol) were placed at the bottom of the liner. The crucible containing KNH_2 (477.2 mg; 8.568 mmol) was then placed on top of these starting materials. After flushing the autoclave three times with ammonia and subsequent cooling, 1.06 mol ammonia was condensed into it (26.5 ml). Then the autoclave was heated to 724 K with a heating rate of 1.43 K/min, kept at this temperature for 150 h and then cooled back down to room temperature with 0.143 K/min. During the reaction a maximum pressure of 2120 bar was observed.

Single crystal X-ray diffraction data collection was performed on a κ-CCD (Bruker Cooperation, Billerica, MA, USA) with Mo-$K_{\alpha1}$ radiation and a CCD detector for the crystals of $[Cr(NH_3)_6][AlF_6]$ and $K_2[Cr(NH_3)_4F_2][Si(NH_3)_{0.5}F_{5.5}]_2$. For the single crystal of $[Cr(NH_3)_5F][SiF_6]$ a StadiVari diffractometer (STOE & Cie GmbH, Darmstadt, Germany) fitted with a Pilatus 200 K detector and Mo-$K_{\alpha1}$ radiation was used. All measurements were performed at room temperature. The crystal structures were then solved and refined using the SHELX-2013 software package.[18] Hydrogen positions for $[Cr(NH_3)_6][AlF_6]$ were taken from the difference Fourier map and refined without constraints. For $[Cr(NH_3)_5F][SiF_6]$ the hydrogen positions can also be extracted from the difference Fourier map, however, refinements do not lead to satisfactory distances and angles within ammine ligands. Thus, in the final refinement a riding model with idealized geometry was applied preventing a reasonable analysis of the hydrogen bond network. For $K_2[Cr(NH_3)_4F_2][Si(NH_3)_{0.5}F_{5.5}]_2$ the disorder prevents the localization of hydrogen atomic positions.

During structural refinements the presence of a pseudomerohedral twin in case of $[Cr(NH_3)_5F][SiF_6]$ with a monoclinic unit cell and an angle close to 90° was apparent. For $K_2[Cr(NH_3)_4F_2][Si(NH_3)_{0.5}F_{5.5}]_2$ a merohedric twin possibly formed by an order-disorder transition from a rotational disordered high-temperature form was encountered. The latter made it necessary to reduce symmetry from *I*4/*mmm* to the lower Laue class *I*4/*m* and introduce a two-fold rotational axis as the twin element. Here we chose a rotational axis along *a* alternative to those along *b* or the respective diagonal.

Information on atomic parameters, displacement parameters and selected interatomic distances are listed in Tables S1–S9 of the supporting information. Further details of the crystal structure investigations may be obtained from the Fachinformationszentrum Karlsruhe, 76344 Eggenstein-Leopoldshafen, Germany (https://www.ccdc.cam.ac.uk/structures/ E-Mail: crysdata@fiz-karlsruhe.de,) on quoting the depository numbers CSD-2177525 for $[Cr(NH_3)_6][AlF_6]$, CSD-2177526 for $[Cr(NH_3)_5F][SiF_6]$ and CSD-2177527 for $K_2[Cr(NH_3)_4F_2][Si(NH_3)_{0.5}F_{5.5}]_2$.

Acknowledgements

We thank Dr. Falk Lissner for collection of X-ray intensity data. This research was funded by the Deutsche Forschungsgemeinschaft (DFG), grant number NI489/16-1. Open Access funding enabled and organized by Projekt DEAL.

Conflict of Interest

The authors declare no conflict of interest.

Data Availability Statement

The data that support the findings of this study are available in the supplementary material of this article.

Keywords: ammonothermal synthesis · chromium · hexafluoridosilicate · hexafluoridoaluminate

[1] a) H. Jacobs, D. Schmidt, *Curr. Top. Mater. Sci.* **1982**, *8*, 381–427; b) T. M. M. Richter, R. Niewa, *Inorganics* **2014**, *2*, 29–78.
[2] a) D. Peters, *J. Cryst. Growth* **1990**, *104*, 411–418; b) R. Dwiliński, A. Wysmołek, J. Baranowski, M. Kamińska, R. Doradziński, J. Garczyński, L. Sierzputowski, H. Jacobs, *Acta Phys. Pol. A* **1995**, *88*, 833–836; c) J. Hertrampf, P. Becker, M. Widenmeyer, A. Weidenkaff, E. Schlücker, R. Niewa, *Cryst. Growth Des.* **2018**, *18*, 2365–2369.
[3] E. Meissner, R. Niewa (Eds.) *Springer series in materials science, Volume 304: Ammonothermal Synthesis and Crystal Growth of Nitrides – Chemistry and Technology*, Springer **2021**.
[4] J. Häusler, W. Schnick, *Chemistry* **2018**, *24*, 11864–11879.
[5] P. Becker, T. B. Cekovski, R. Niewa, *Crystals* **2021**, *11*, 679.
[6] C. Bäucker, P. Becker, K. J. Morell, R. Niewa, *Inorganics* **2022**, *10*, 7.
[7] K. Wieghardt, J. Weiss, *Acta Crystallogr. Sect. B* **1972**, *28*, 529–534.
[8] K. Wieghardt, H. Siebert, *J. Mol. Struct.* **1971**, *7*, 305–313.
[9] D. June Sutor, *Nature* **1962**, *195*, 68–69.
[10] A. Bondi, *J. Phys. Chem.* **1964**, *68*, 441–451.
[11] a) J. V. Brenčič, B. Čeh, I. Leban, *Monatsh. Chem.* **1981**, *112*, 1359–1368; b) D. Göbbels, G. Meyer, *Z. Anorg. Allg. Chem.* **2000**, *626*, 1499–1500.
[12] C. Plitzko, G. Meyer, *Z. Anorg. Allg. Chem.* **1996**, *622*, 1646–1650.
[13] J. A. A. Ketelaar, *Z. Kristallogr.* **1935**, *92*, 155–156.
[14] N. Alt, E. Meissner, E. Schlücker, L. Frey, *Phys. Status Solidi C* **2012**, *9*, 436–439.
[15] N. S. Alt, E. Meissner, E. Schluecker, *J. Cryst. Growth* **2012**, *350*, 2–4.
[16] B. Hertweck, S. Schimmel, T. G. Steigerwald, N. S. Alt, P. J. Wellmann, E. Schluecker, *J. Supercrit. Fluids* **2015**, *99*, 76–87.
[17] G. F. Hüttig, *Z. Anorg. Allg. Chem.* **1920**, *114*, 161–173.
[18] a) G. M. Sheldrick, *Acta Crystallogr. Sect. A* **2008**, *64*, 112–122; b) G. M. Sheldrick, *Acta Crystallogr. Sect. C* **2015**, *71*, 3–8.

Manuscript received: June 17, 2022
Revised manuscript received: August 2, 2022
Accepted manuscript online: August 6, 2022

